The de Haas-van Alphen effect of the stage-1 $AlCl_3$ graphite intercalation compound

1994 J. Phys.: Condens. Matter 6 3031

(http://iopscience.iop.org/0953-8984/6/16/008)

J. Phys.: Condens. Matter 6 (1994) 3031–3038. Printed in the UK

The de Haas–van Alphen effect of the stage-1 $AlCl_3$ graphite intercalation compound

T R Chien, D Marchesan, P K Ummat and W R Datars

Department of Physics and Astronomy, McMaster University, Hamilton, Ontario L8S 4M1, Canada

Received 14 November 1993, in final form 28 January 1994

Abstract. The de Haas–van Alphen (DHVA) effect of the stage-1 $AlCl_3$ graphite intercalation compound has been studied in the temperature range from 1.5 K to 4.2 K with magnetic fields of 2.5 to 5 T. There is a dominant oscillation with a frequency of 1250 T with the magnetic field parallel to the c axis, which corresponds to an extremal cross sectional Fermi surface area of 0.119 $Å^{-2}$. The charge transfer per C atom is $0.032e^+$. The cyclotron mass is $(0.261 \pm 0.001)\, m_0$. The Fermi energy determined from the Holzwarth band model is -1.14 eV. No beating of the dominant frequency is observed in the 2.5 to 5 T field range, which indicates little undulation of the Fermi surface along the c axis. The Dingle temperature T_D of one sample is (3.1 ± 0.2) K, which corresponds to a mean free path l_D of $(4.8 \pm 0.4) \times 10^3$ Å.

1. Introduction

Graphite intercalation compounds (GICs) can be synthesized by inserting layers of molecules or atoms of different chemical species between the graphite layers [1]. Different staging of the GICs can be formed for different chemicals and different synthesizing conditions. Charge transfer from the intercalants to the C atoms makes the GICs very good metals and some donor-type GICs such as C_8K are superconductors. The intercalation of $AlCl_3$ forms an acceptor-type stage-1 GIC with alternating $AlCl_3$ and C layers.

The low charge transfer per C atom ($< 0.1e$) only perturbs the single-layer graphitic π-band weakly. The interaction between adjacent C layers is weak because of the tight binding of charge to the acceptors. Therefore the band structure is two dimensional (2D) in nature, similar to that of a single graphite layer. The Fermi surface (FS) of the 2D system is essentially a straight cylinder with its axis along the c axis. A small interlayer interaction causes an undulation of the FS along the c axis and makes the GIC less 2D.

A theoretical band structure of a stage-1 acceptor GIC was developed by Holzwarth [2] using the linear combination of atomic orbitals (LCAO) method. The calculation included four intralayer interactions and four interlayer interactions (for higher-stage GICs). The energy difference of the non-equivalent intralayer C sites was included. Because of its complexity, analytical solutions could not be solved and numerical calculations were needed in general. A simpler theory by Blinowski *et al* [3] used a tight-binding model, which took into account only the nearest-neighbour intralayer interactions. It gave a first-order expansion of energy versus momentum dispersion near the corners (U and U′ points) of the hexagonal Brillouin zone (BZ). Since the magnitude of the Fermi vector k_F was only about 10% of that of k_U of the BZ, the Blinowski model gave a good approximation of the band structure of the stage-1 GIC.

0953-8984/94/163031+08$19.50

The de Haas–van Alphen (DHVA) effect can be observed in the GIC made from highly oriented pyrolitic graphite (HOPG) or single-crystal graphite [1]. The DHVA measurements give a direct mapping of the extremal cross section of the FS perpendicular to the field direction. In this paper, we measured the DHVA effect of the stage-1 $AlCl_3$ GIC with an AC modulation technique [4]. One dominant oscillation with a frequency of 1250 T was observed; this is similar to those of the other stage-1 acceptor GICs [5–9]. More details will be discussed in the following sections.

2. Experimental details

The stage-1 $AlCl_3$ GIC was made from HOPG. Slabs of the HOPG were first cut into pieces with typical dimensions of $1.5 \times 1.5 \times 0.6$ mm^3. The surfaces of the HOPG were peeled off and cleaned with pure acetone in an ultrasonic cleaner for 5 min. The dried HOPG was put into a sealed pyrex tube with 99.99% pure anhydrous $AlCl_3$ powder and approximately 600 Torr ultra-high-purity Cl_2. The sealed reaction tube was put into an oven and the intercalation of the compound took place at 180 °C for 72 h [10–12]. After the reaction, the resulting stage-1 $AlCl_3$ GIC was dark blue, shiny, soft and air sensitive. The nominal composition of our samples was $C_{7.5}AlCl_3$, determined by the weight up take from intercalation.

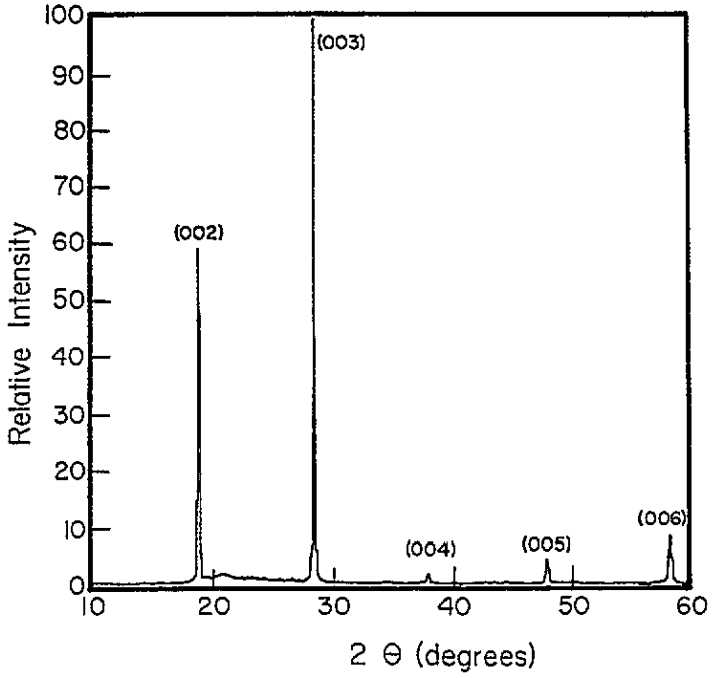

Figure 1. (00*l*) x-ray diffraction of the stage-1 $AlCl_3$ GIC with Cu Kα radiation.

The (00*l*) x-ray diffraction pattern with Cu Kα radiation, obtained with the sample in a leak-tight holder, is shown in figure 1. The diffraction peaks are indexed from (002) to (006), with the (003) peak the most intense one. No diffraction from other stages or from graphite is observed. The *c*-axis repeat distance I_c is 9.50 Å, which is consistent with previous results [11–13].

The DHVA signals were detected with the AC modulation technique [4]. The detection

coils for the DHVA experiments consisted of a balance coil wound on top of a pick-up coil. The exact number of turns on the balance coil was determined by minimizing the null AC signal from the two coils.

The detection coil set could be taken from the probe so that the sample could be loaded into the pick-up coil in a dry box. Two Kel-F plugs in the ends of the pick-up coil sealed the stage-1 $AlCl_3$ GIC from exposure to air. The c axis of the sample was along the coil axis, as was the field of a 5.5 T superconducting solenoid. The sample and the coils were slowly cooled down to 100 K from room temperature in 36 h before further cooling down to 4.2 K.

The DHVA experiments were performed below 4.23 K with a slowly varying field in the range of 2.5–5 T. The AC modulation was 47 Hz with a typical modulation field of 27.5 G RMS along the DC field direction, and the second harmonic (94 Hz) of the DHVA signal was detected and recorded as a function of field. In order to determine the cyclotron mass, the temperature dependence of the DHVA amplitude was measured at temperatures between 2.5 K and 4.2 K with the temperatures determined from the He vapour pressure.

3. Experimental results

The DHVA oscillations with the field H parallel to the c axis are shown in figure 2. The temperature was 1.81 K and the sample had been thermally cycled once before the measurement. No beating effect was observed in the field range 2.5–4 T and the envelope increased monotonically with field. A small quasi-periodic variation on top of the growing envelope was present. This same effect was also observed in stage-1 C_8K [14].

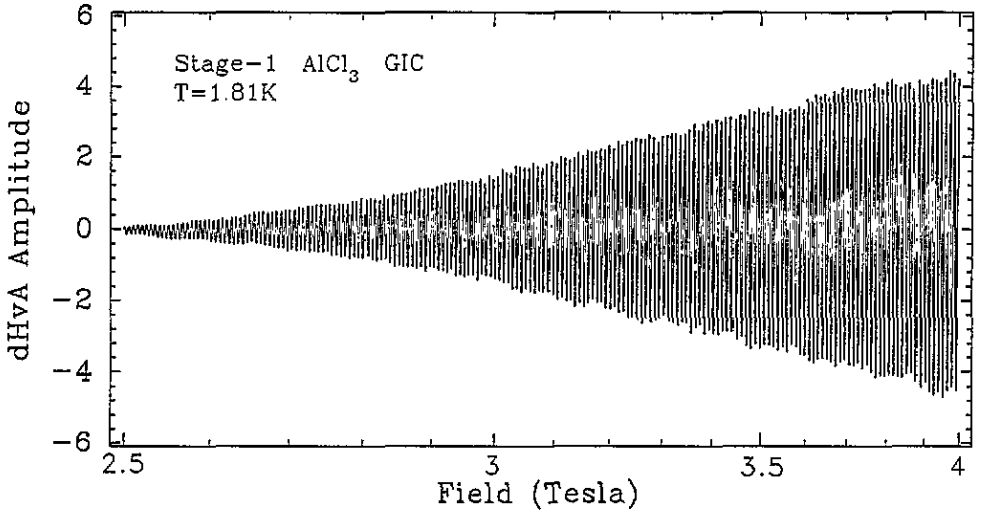

Figure 2. DHVA oscillations of the stage-1 $AlCl_3$ GIC taken at the second harmonic of the modulation field of 47 Hz for fields between 2.5 and 4 T. The temperature was 1.81 K. The field H and the modulation field were parallel to the c axis of the sample. This plot was generated by a computer with 1024 digitized data points.

The Fourier spectrum of the DHVA oscillation of figure 2 is shown in figure 3. There is one DHVA frequency F at 1250 T with a width of 15 T. The second harmonic $2F$ at 2500 T (not shown) was very small. The Fourier transformation did not pick up the small variation

of the growing envelope. This indicated the non-periodic nature of the small variation. The inset in figure 3 shows the Fourier spectrum of the same sample after the first cooling from 300 K. The small peak at 1155 T is a frequency that disappears on thermal cycling.

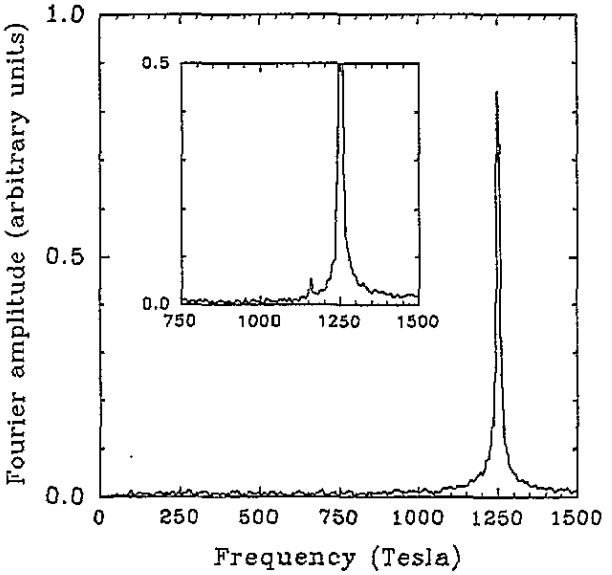

Figure 3. The Fourier amplitude versus frequency from the Fourier transform of the DHVA oscillations in figure 2. The sample had been slowly cooled down from room temperature twice. The inset shows the Fourier spectrum of the same sample after the first cooling down.

The angular dependence of the Fourier frequency F was measured with a rotatable pick-up coil. Data were taken every 2° from $\theta = 0°$ where θ is the angle between the c axis and the field direction. The frequency was determined by a Lorentzian fit to the Fourier spectrum at each angle. The Fourier frequency was expected to scale as $F(\theta) \propto \sec(\theta)$ for a cylindrical Fermi surface. Such an angular dependence was observed within the experimental uncertainty for $0° < \theta < 10°$ before the DHVA signal vanished at larger angles.

The temperature dependence of the Fourier amplitude, amplitude(T), provided a measure of the cyclotron mass m_c. For the same field range at each temperature,

$$\text{Fourier amplitude}(T) \propto T / \sinh\left[b \left(\frac{m_c}{m_0} \right) T/H \right] \tag{1}$$

where $b = 2\pi^2 k_B m_0 / e\hbar = 14.693\,\text{T K}^{-1}$, k_B is the Boltzmann constant and m_0 is the free electron mass. Equation (1) is derived from the Lifshitz–Kosevich theory [15]. The Fourier amplitude versus temperatures for oscillations observed in the field range of 4–5 T is shown by open circles in figure 4. The solid curve is a least-χ^2 fit to equation (1) with $H = 4.444\,44$ T, the field of the average of the reciprocal field range 0.25–0.2 T^{-1}. The best-fit m_c value is $(0.261 \pm 0.001)\, m_0$.

In order to determine the field dependence of the DHVA amplitude an extra factor for the AC modulation has to be added to the standard Lifshitz–Kosevich formula [4]. With the second-harmonic (2×47 Hz) detection scheme, the multiplying factor is $-4\omega J_2(\lambda)$, where $J_2(\lambda)$ is a Bessel function of the first kind, $\omega = 2\pi \times 47$, $h \sin \omega t$ is the AC modulation field and $\lambda = 2\pi F h / H^2$. When the phase factor is ignored, the detected DHVA amplitude at 2ω

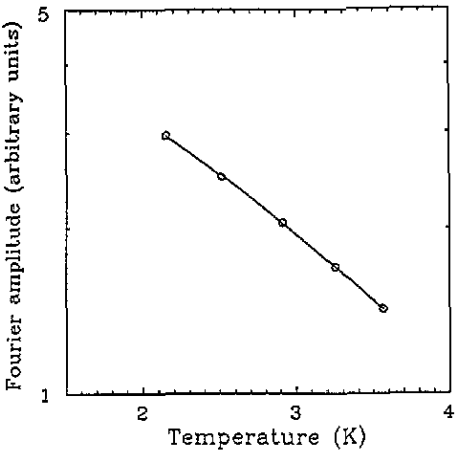

Figure 4. The Fourier amplitude versus temperature of the 1250 T frequency for the field range from 4 to 5 T. The solid curve is a least-χ^2 fit to equation (1). The best-fit $m_c = (0.261 \pm 0.001)m_0$.

is

$$\text{amplitude} \propto \frac{\partial \tilde{M}(H)}{\partial t} \propto \sqrt{H}\left[\frac{b(m_c/m_0)T/H}{\sinh(b(m_c/m_0)T/H)}\right]\exp\left(-b\left(\frac{m_c}{m_0}\right)T_D/H\right)J_2(\lambda) \quad (2)$$

where $b = 14.693\ \mathrm{T\,K^{-1}}$ was defined previously and T_D is the Dingle temperature. The term in the square brackets is the thermal smearing factor and the exponential term is the Dingle reduction factor due to a finite scattering rate with defects, impurities or magnetic moments. Equation (2) reduces to equation (1) for a fixed field range.

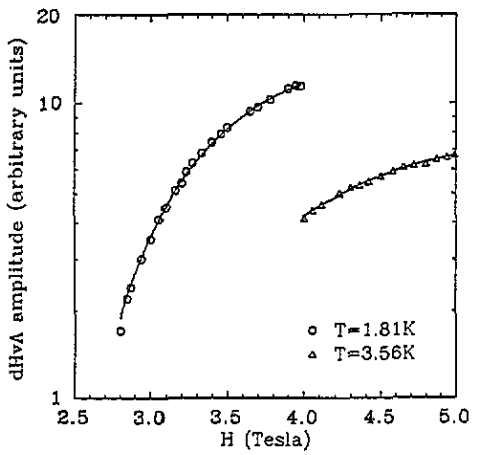

Figure 5. The DHVA amplitude versus the applied magnetic field H for two different temperatures and field ranges. The solid curves are least-χ^2 fits to equation (2). The Dingle temperature for this sample is (3.1 ± 0.2) K.

The Dingle temperature T_D can be abstracted from the field dependence of the DHVA amplitude (shown in figure 2) because the amplitude increased with field with no beating. Figure 5 shows the DHVA amplitude versus field H for two different temperatures and field ranges. The solid curves are the least-χ^2 fit of the data points to equation (2)

with $h = 0.0039$ T and $F = 1250$ T. The best-fit T_D values are (3.15 ± 0.2) K and (3.05 ± 0.1) K for the data at 1.81 K and 3.56 K, respectively. The relaxation time constant $\tau_D = \hbar/(2\pi k_B T_D) = (3.9 \pm 0.3) \times 10^{-13}$ s and the mean free path $l_D = \tau_D v_F = \tau_D \sqrt{-2E_F/m_c} = (4.8 \pm 0.4) \times 10^3$ Å for the average $T_D = (3.1 \pm 0.2)$ K.

In some samples, a dominant DHVA frequency between 420 T and 520 T was observed with its DHVA signal more than two orders of magnitude weaker than the dominant amplitude of a sample with the 1250 T frequency. The conductivity was also more than one order of magnitude lower from penetration depth measurements. The measured cyclotron mass for the low frequency was $(0.17 \pm 0.02)\, m_0$. The x-ray diffraction of these samples was not significantly different from figure 1 and indicated no structural change. Previous studies on other stage-1 acceptor GICs [5–8] also showed a lower DHVA frequency between 300 T and 600 T with a cyclotron mass of about $0.17\, m_0$. These lower frequencies indicate a smaller charge transfer ($\approx 0.01e^+$ per C atom) in all or part of these samples. Such a hypothetical explanation (for the lower frequency) can also account for the lower conductivity in the stage-1 $AlCl_3$ GIC samples with a lower frequency since less charge is transfered into the conduction band. The microscopic origin for the presence of the lower frequency is not understood at the present time.

4. Discussion

The FS of the stage-1 GIC is essentially a straight cylinder at each corner of the hexagonal BZ with the FS extremal area $A_e = (2\pi e/\hbar)F = 0.119\,\text{Å}^{-2}$ for $F = 1250$ T. The Holzwarth model gives a more accurate description than the Blinowski model because the interaction energies between non-equivalent, in-plane C sites are not neglected. By choosing an appropriate linear combination of interlayer wavefunctions and matrix elements [16] in the Holzwarth model, the FS parameters can be calculated as a function of Fermi energy E_F by solving the 2×2 Hamiltonian matrix elements by a numerical method. The area of $0.119\,\text{Å}^{-2}$ is obtained with $E_F = -1.14$ eV [17]. The cyclotron mass m_c for this Fermi energy is $0.274\, m_0$ and is in reasonable agreement with the measured value $(0.261 \pm 0.001)\, m_0$.

Assuming the Fermi contour in the graphite plane to be circular, the radius k_F of the Fermi circles (from U or U′ points) is equals to $\sqrt{A_e/\pi} = 0.195\,\text{Å}^{-1}$. Thus $k_F/k_U = 0.115$ and the Blinowski model is also a valid description for the stage-1 $AlCl_3$ GIC.

In the Blinowski model for the stage-1 acceptor compound, the E_F is related to A_e by

$$E_F = -\frac{\sqrt{3}\,a}{2}\,\gamma_0(A_e/\pi)^{1/2} \tag{3}$$

the cyclotron mass m_c is

$$m_c \equiv \frac{\hbar^2}{2\pi}\left[\frac{\partial A_e}{\partial E}\right]_{E_F} = \frac{4\hbar^2}{3a^2}(-E_F/\gamma_0^2) \tag{4}$$

and the charge transfer per C atom is

$$f/l = \frac{\sqrt{3}\,a^2}{4\pi^2}\,A_e \tag{5}$$

where $a = 2.46$ Å is the length of the primitive lattice translation vector, γ_0 is the nearest-neighbour intralayer interaction energy term and $\hbar$ is the Planck constant. Equation (5) is only valid for the basic graphitic band.

With the experimental values $m_c = (0.261 \pm 0.001)\, m_0$ and $A_e = 0.119\,\text{Å}^{-2}$, γ_0 is calculated to be 2.67 eV from equations (3) and (4). The Fermi energy E_F is then -1.11

eV and f/l, the charge transfer per C atom, is 0.0316. The $E_F = -1.11$ eV in the Blinowski model is consistent with $E_F = -1.14$ eV in the Holzwarth model within 3%. Both models give a good description of the band structure of the stage-1 $AlCl_3$ GICs.

Previous DHVA work with stage-1 acceptor GIC include intercalants such as AsF_5 [5], $SbCl_5$ [6], SbF_6^- [7], $SbCl_4F$ [8] and $CdCl_2$ [9]. The DHVA frequency from the graphitic π bands in these compounds is in the range 1140–1630 T. The cyclotron mass m_c and the Fermi energy magnitude increase with the DHVA frequency. All of the samples agree well with the Holzwarth and the Blinowski model within a few per cent. Thus the electronic properties of these compounds are very similar.

No beating effect was observed in the stage-1 $AlCl_3$ GIC which indicated no fine splitting of the 1250 T frequency. Compared with the stage-1 $CdCl_2$ GIC which has a frequency splitting of 50 T [9], the stage-1 $AlCl_3$ GIC has little interlayer interaction to split the frequency and therefore is more 2D than the stage-1 $CdCl_2$ GIC.

One thing worth noting is that the Dingle temperature after the sample was cooled for the first time is (2.2 ± 0.2) K, less than the value of (3.1 ± 0.2) K after subsequent cooling cycles. This indicates less electron scattering with a longer relaxation time and may explain why the small peak at 1155 T in the Fourier spectrum is present in the inset of figure 3. If there were regions or domains with a slightly different c-axis repeat distance, they would have a different FS cross sectional area and could be resolved only with the longer relaxation time after the first cooling. Electron scattering may be increased enough after subsequent cooling cycles to make these regions unobservable.

5. Conclusions

The dHvA oscillation frequency of the stage-1 $AlCl_3$ GIC is 1250 T with the magnetic field parallel to the c axis. The cyclotron mass for this frequency is $(0.261 \pm 0.001)\,m_0$. The FS is a straight cylinder with a cross sectional area of 0.119 Å at each corner of the hexagonal Brillouin zone. No undulation of the Fermi surface along the c axis is observed. The Blinowski model is a valid description for the stage-1 $AlCl_3$ GIC since $k_F/k_U = 0.115$ and the linear dispersion relation holds. $\gamma_0 = 2.67$ eV and $E_F = -1.11$ eV in the Blinowski model and f/l, the charge transfer per C atom, is 0.0316. The Fermi energy E_F calculated from the Holzwarth model is -1.14 eV and the cyclotron mass m_c is calculated to be $0.274\,m_0$. Both models give a consistent description of the band structure of the stage-1 $AlCl_3$ GIC. The Dingle temperature T_D of one sample is (3.1 ± 0.2) K, which corresponds to a mean lifetime $\tau_D = (3.9 \pm 0.3) \times 10^{-13}$ s and a mean free path $l_D = (4.8 \pm 0.4) \times 10^3$ Å. For some samples, a dominant peak between 420 T and 520 T is observed with a DHVA amplitude more than two orders of magnitude weaker. The cyclotron mass for this band is $(0.17 \pm 0.02)\,m_0$. The microscopic origin for the presence of the lower frequency is not understood at the present time.

Acknowledgments

We like to thank Mr T Olech for his participation in the construction of the probe. The HOPG was kindly provided by Dr A W Moore. This research was supported by the Natural Sciences and Engineering Council of Canada.

References

[1] Dresselhaus M S and Dresselhaus G 1981 *Adv. Phys.* **30** 139–326
[2] Holzwarth N A W 1980 *Phys. Rev.* B **21** 3665
[3] Blinowski J, Hau N H, Rigaux C, Vieren J P, Le Toullec R, Furdin G, Hérold A and Melin J 1980 *J. Physique* **41** 47–58
[4] Shoenberg D and Stiles P J 1964 *Proc. R. Soc.* A **281** 62
[5] Markiewicz R S, Hart H R Jr., Interrante L V and Kasper J S, 1980 *Solid State Commun.* **35** 513
[6] Zaleski H, Ummat P K and Datars W R 1984 *J. Phys. C: Solid State Phys.* **17** 3167–72
[7] Zaleski H, Ummat P K and Datars W R 1985 *Synth. Met.* **11** 183–91
[8] Zaleski H, Ummat P K and Datars W R 1989 *J. Phys.: Condens. Matter* **1** 369–73
[9] Datars W R, Ummat P K, Aoki H and Uji S 1993 *Phys. Rev.* B **48** 18 174
[10] Dzurus M L and Hennig G R 1957 *Graphite Compounds* **79** 1051
[11] Bach B and Ubbelohde A R 1971 *Proc. R. Soc.* A **325** 437–45
[12] Hooley J G, 1975 *Carbon* **13** 469–71
[13] Vangelisti R, Nadi N and Lelaurain M 1983 *Synth. Met.* **7** 297–304
[14] Wang G, Datars W R and Ummat P K 1991 *Phys. Rev.* B **44** 8294
[15] Lifshitz I M and Kosevich A M *1956 Sov. Phys.–JETP 2 636*
[16] The intralayer matrix elements were chosen from table I of [2].
[17] Zaleski H 1985 *Ph D Thesis* McMaster University